NASA
Technical
Paper
2111

January 1983

Elastohydrodynamic Lubrication of Rectangular Contacts

Bernard J. Hamrock
and Bo O. Jacobson

NASA

NASA
Technical
Paper
2111

1983

Elastohydrodynamic Lubrication of Rectangular Contacts

Bernard J. Hamrock
and Bo O. Jacobson
Lewis Research Center
Cleveland, Ohio

NASA
National Aeronautics
and Space Administration

**Scientific and Technical
Information Branch**

SUMMARY

A procedure for the numerical solution of the complete isothermal elastohydrodynamic lubrication problem for rectangular contacts is outlined. This procedure calls for the simultaneous solution of the elasticity and Reynolds equations. In the elasticity analysis the conjunction is divided into equal rectangular areas. It is assumed that a uniform pressure is applied over each area. In the numerical analysis of the Reynolds equation the parameter $\Phi = QH^{3/2}$ is introduced in order to help the relaxation process. The analysis couples the elasticity and Reynolds equations, going from the inlet to the outlet without making any assumptions other than neglecting side leakage.

By using the procedures outlined in the analysis the influence of the dimensionless speed U, load W, and materials G parameters on minimum film thickness is investigated. Ten cases are used to generate the minimum-film-thickness relationship.

$$\overline{H}_{min} = 3.07\ U^{0.71}G^{0.57}W^{-0.11}$$

The most dominant exponent occurs in association with the speed parameter; the exponent on the load parameter is very small and negative. The materials parameter also carries a significant exponent, although the range of the parameter in engineering situations is limited. The five dimensionless speed parameter values used in obtaining the preceding equation are varied over a range six times the lowest speed value. The four dimensionless load values are varied over a range 1.8 times the lowest load value. Conditions corresponding to the use of solid materials of bronze and steel and lubricants of paraffinic and naphthenic mineral oils are considered in obtaining the exponent in the dimensionless materials parameter.

Plots are presented that indicate in detail the pressure distribution, film shape, and flow within the contact. The characteristic pressure spike is clearly in evidence as is the parallel film shape through the central portion of the contact. Minimum film thickness occurs near the outlet of the contact.

INTRODUCTION

The recognition and understanding of elastohydrodynamic lubrication represents one of the major developments in the field of tribology in the twentieth century. The revelation of a previously unsuspected regime of lubrication not only explained the remarkable physical action responsible for the effective lubrication of many nonconformal machine elements like gears and rolling-element bearings, but also brought order to the complete spectrum of lubrication regimes, ranging from boundary to hydrodynamic.

Historically one of the first to study the effect of elastic distortion in highly loaded contacts was Meldahl (ref. 1). He examined the effect of high load on film shape and pressure distribution for a constant-viscosity lubricant. The first attempt to analyze both elastic and viscous effects in elastohydrodynamically lubricated contacts was done by Grubin and Vinogradova (ref. 2), who managed to incorporate both the effects of elastic deformation and the viscosity-pressure characteristics of the lubricant in the inlet analysis of hydrodynamic lubrication of nonconformal contacts. Their work dealt mostly with a line contact, and it was assumed that the shape of the elastically deformed solids in highly loaded lubricated contacts was the same as the shape produced in dry (Hertzian) contacts. This assumption facilitated the

solution of the Reynolds equation in the inlet region of the contact and enabled the separation of the solids in the central region of the contact to be determined with commendable accuracy.

Dowson and Higginson (ref. 3) obtained an empirical formula for the isothermal-line-contact elastohydrodynamic lubrication problem. This formula showed the effect of speed, load, and material properties on minimum film thickness and was based on their theoretical solutions. In the procedure they adopted, the computed film shape was compared with the shape of the elastically deformed solids, and then the pressure curve was modified to improve the agreement between the two shapes. These calculations were performed on hand-operated desk calculating machines. Jacobson (ref. 4) solved the elastohydrodynamic lubrication problem for a spherical contact under pure rolling conditions and a non-Newtonian lubricant with a limiting shear strength. The shear strength of the lubricant limited the pressure gradients and shear stresses in the oil. Therefore no pressure spikes were seen in the theoretical solutions.

Hamrock and Dowson (ref. 5) were able to successfully obtain a theoretical approach to coupling the elasticity equation with the Reynolds equation for elliptical contacts such as those normally found in gears and ball bearings. Hamrock and Dowson's work on elastohydrodynamic lubrication (ref. 6) considered the complete spectrum of contact geometries (ranging from point to line contacts), materials (hard and soft), and lubricant availability (fully flooded or starved conditions).

To obtain a better understanding of the failure mechanism in machine elements, the next generation of elastohydrodynamic lubrication analysis should incorporate such effects as

(1) Surface roughness effects
(2) Non-Newtonian effects
(3) Temperature effects

The foundation studies that produced the complete elastohydrodynamic lubrication solutions for rectangular contacts given in the present report will be used in further studies incorporating these effects. To incorporate these effects in an initial study, rectangular contact analysis, often referred to as "line" or "one dimensional" contact analysis, should be used instead of elliptical contact analysis because of the added complexity of considering these effects.

The analysis in the present report couples the elasticity and Reynolds equations, going from the inlet to the outlet without making any assumptions other than neglecting side leakage. This analysis may thus be used as the foundation for the more complicated analysis incorporating surface roughness effects, non-Newtonian effects, and temperature effects.

In the results the influence of dimensionless speed, load, and materials parameters on minimum film thickness was investigated for a contact fully immersed in lubricant (i.e., fully flooded). The dimensionless speed and load parameters were varied over a range of 11 and 2-1/2 times, respectively. Conditions equivalent to using solid materials of bronze and steel and lubricants of paraffinic and naphthenic mineral oils were considered in obtaining the exponent on the dimensionless materials parameter. Ten cases were used in obtaining the fully flooded film thickness formula. A fully flooded condition is said to exist when the inlet distance of the contact ceases to influence the minimum film thickness in any significant way. The inlet distance of the contact is defined as the distance from the center of the contact to the edge of the computing area. Besides the film thickness calculations that were made, calculation of the force components, shear forces, coefficient of fric-

tion, and center of pressure were also performed. A simple formula is provided that described the location of the center of pressure relative to the inlet of the contact and as a function of the dimensionless load and speed parameters for steel surfaces.

Computer plots are presented that indicate in detail the pressure spike and minimum film thickness. Plots are also shown of the parallel shape of the reduced pressure, the Poiseuille term, and the mass flow per unit length within the contact.

SYMBOLS

A	constant defined in eq. (27)
B	$\overline{b}/b$
b	semiwidth of Hertzian contact, $2R\sqrt{2W/\pi}$, m
$\overline{b}$	b/n, m
C	constant defined in eq. (28)
$C_1,\ldots,C_6$	constants
D	defined by eq. (19)
E	modulus of elasticity, N/m^2
E'	effective elastic modulus, $2/\{[(1 - \nu_a^2)/E_a] + [(1 - \nu_b^2)/E_b]\}$, N/m^2
F	dimensionless shear force
f	shear force per unit length, N/m
G	dimensionless materials parameter, $\alpha E'$
H	dimensionless film thickness, h/R
H_{min}	dimensionless minimum film thickness, h_{min}/R
$\overline{H}_{min}$	dimensionless minimum film thickness obtained from least-squares fit of data
$(\overline{H}_{min})_D$	dimensionless minimum film thickness obtained from Dowson (ref. 7)
$(\overline{H}_{min})_{DH}$	dimensionless minimum film thickness obtained from Dowson and Higginson (ref. 3).
H_o	dimensionless constant defined in eq. (23)
h	film thickness, m

h_{min}	minimum film thickness, m
K	dimensionless mass flow per unit length
k	mass flow per unit length, kg/(s m)
L	constant defined in eq. (29)
M	constant defined in eq. (30)
n	*number of nodes in semi-axis of contact*
P	dimensionless pressure, p/E'
p	pressure, N/m^2
Q	dimensionless reduced pressure, q/E'
q	reduced pressure, N/m^2
R	effective radius in x-direction, m
r	curvature radius, m
S	geometrical separation, m
T	defined in eq. (67)
U	dimensionless speed parameter, $\eta_0 u/E'R$
u	surface velocity in direction of motion, $(u_a + u_b)/2$, m/s
V_1	$(\overline{H}_{min} - H_{min})\ 100/H_{min}$
V_2	$[(\overline{H}_{min})_D - \overline{H}_{min}]100/\overline{H}_{min}$
W	dimensionless load parameter, $w_z/E'R$
w	load, N/m
X	dimensionless coordinate, x/b
X_{cp}	location of dimensionless center of pressure, x_{cp}/b
x	coordinate in direction of motion, m
x_{cp}	location of center of pressure, m
z	coordinate in direction of film thickness, m
α	pressure-viscosity coefficient of lubricant, m^2/N
γ	angle defined in eq. (43)
δ	elastic deformation, m

ε	coefficient of determination
η	absolute viscosity at gage pressure, (N s)/m^2
$\bar{\eta}$	dimensionless viscosity, η/η_0
η_0	viscosity at atmospheric pressure, (N s)/m^2
μ	coefficient of friction
ν	Poisson's ratio
ρ	lubricant density, kg/m^3
$\bar{\rho}$	dimensionless density, ρ/ρ_0
ρ_0	density at atmospheric pressure, kg/m^3
Φ	$QH^{3/2}$

Subscripts:

a	solid a
b	solid b
x	coordinate in direction of motion
z	coordinate in direction of film thickness

THEORY

Reynolds Equation

The general approach to the numerical solution of the one-dimensional rectangular or line-contact problem covered in this report is similar to the method used by Hamrock and Dowson (ref. 5) in solving the two-dimensional elliptical contact problem in elastohydrodynamic lubrication. The Reynolds equation for one-dimensional flow where side leakage is neglected can be written as

$$\frac{d}{dx}\left(\frac{\rho h^3}{\eta}\frac{dp}{dx}\right) = 12u\frac{d(\rho h)}{dx} \tag{1}$$

where $u = (u_a + u_b)/2$ is the mean surface velocity or the entraining velocity in the x-direction.

Letting

$$X = x/b,\ \bar{\rho} = \rho/\rho_0,\ \bar{\eta} = \eta/\eta_0,\ H = h/R,\ \text{and}\ P = p/E' \tag{2}$$

where

$$\frac{1}{R} = \frac{1}{r_a} + \frac{1}{r_b} \tag{3}$$

$$E' = \frac{2}{\frac{1 - \nu_a^2}{E_a} + \frac{1 - \nu_b^2}{E_b}} \tag{4}$$

equation (1) can be rewritten in dimensionless form as

$$\frac{d}{dx}\left(\frac{\bar{\rho}\bar{H}^3}{\bar{\eta}} \frac{dP}{dx}\right) = 24U \sqrt{\frac{2W}{\pi}} \frac{d}{dx} (\bar{\rho}\bar{H}) \tag{5}$$

where

$$U = \frac{u\eta_0}{E'R} \tag{6}$$

is the dimensionless speed parameter,

$$W = \frac{w_z}{E'R} \tag{7}$$

is the dimensionless load parameter, and w_z is the load per unit width.

Figure 1 shows the radius of the rollers used in defining equation (3). It is assumed that convex surfaces, as shown in figure 1, exhibit positive curvature and concave surfaces, negative curvature. Therefore, if the center of the curvature lies within the solid, the radius of curvature is positive; if the center of curvature lies outside the solid, the radius of curvature is negative.

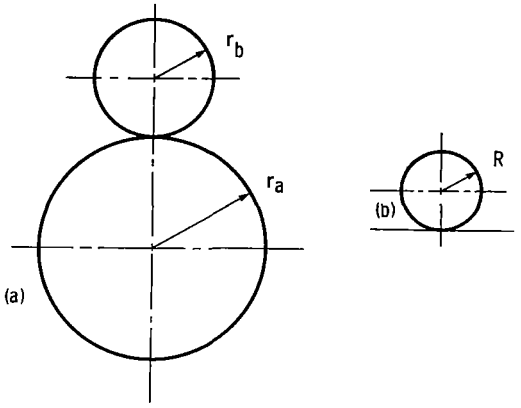

(a) Two undeformed rollers.
(b) Equivalent cylindrical solid near plane.

Figure 1. - Rollers and equivalent roller.

The viscosity of a fluid may be associated with the resistance to flow, with the resistance arising from intermolecular forces and internal friction as the molecules move past each other. Because of the large pressure variation in the lubricant films the viscosity of the lubricant is not constant in elastohydrodynamically lubricated contacts. Barus (ref. 8) proposed the following formula for the isothermal viscosity-pressure dependence of liquids:

$$\eta = \eta_0 e^{\alpha p} \tag{8}$$

In dimensionless form this equation can be written as

$$\bar{\eta} = \frac{\eta}{\eta_0} = e^{GP} \tag{9}$$

where

$$G = \alpha E' \tag{10}$$

is the dimensionless materials parameter.

Substituting equation (9) into equation (5) gives

$$\frac{d}{dx}\left(\bar{\rho}H^3 e^{-GP} \frac{dP}{dx}\right) = 24U \sqrt{\frac{2W}{\pi}} \frac{d}{dx}(\bar{\rho}H) \tag{11}$$

Grubin and Vinogradova (ref. 2) were the first to introduce the writing of the pressure and viscosity in terms of a reduced pressure as

$$Q = \frac{q}{E'} = \frac{1}{G}(1 - e^{-GP}) \tag{12}$$

and

$$\frac{dQ}{dx} = e^{-GP} \frac{dP}{dx} \tag{13}$$

Note that, as $P \to \infty$, $Q \to 1/G$. Substituting equation (13) into equation (11) gives

$$\frac{d}{dx}\left(\bar{\rho}H^3 \frac{dQ}{dx}\right) = 24U \sqrt{\frac{2W}{\pi}} \frac{d}{dx}(\bar{\rho}H) \tag{14}$$

Density

For a comparable change in pressure the density change is small as compared with the viscosity change. However, very high pressures exist in elastohydrodynamic films, and the liquid can no longer be considered as an incompressible medium. From Dowson and Higginson (ref. 9) the dimensionless density for mineral oil can be written as

$$\bar{\rho} = \frac{\rho}{\rho_0} = 1 + \frac{0.6\ E'P}{1 + 1.7\ E'P} \tag{15}$$

where E' is given in gigapascals.

Film Shape

The film shape can be written simply as

$$h(x) = h_0 + S(x) + \delta(x) \tag{16}$$

where

h_0 constant

$S(x)$ separation due to geometry of undeformed solids

$\delta(x)$ elastic deformation

The separation due to the geometry of the two undeformed rollers shown in figure 1(a) can be described by an equivalent cylindrical solid near a plane, as shown in figure 1(b). The geometrical requirement is that the separation of the two rollers in the initial and equivalent situations should be the same at equal values of x. Therefore using the parabolic approximation we can write the separation due to the undeformed geometry of the two rollers as

$$S(x) = \frac{x^2}{2R} \tag{17}$$

Figure 2 shows a rectangular area of uniform pressure width $2\bar{b}$. From Timoshenko and Goodier (ref. 10) the elastic deformation at a point $\bar{x}$ on the surface of a semi-infinite solid subjected to a pressure p at the point x_1 can be written as

$$\delta(\bar{x}) = \frac{-2}{\pi E'} \int_{-\bar{b}}^{\bar{b}} p \ln (\bar{x} - x_1)^2 \, dx_1 \tag{18}$$

Since the pressure is assumed to be uniform over the rectangular area, the pressure can be put in front of the integral. The integration of equation (18) then results in the following:

$$\delta(\bar{x}) = \frac{2}{\pi} PD \tag{19}$$

where

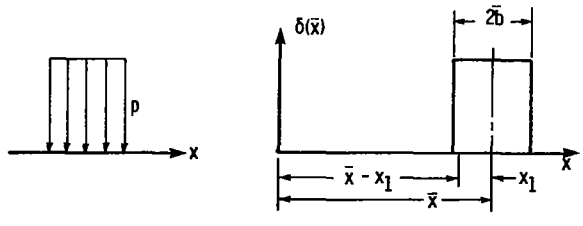

Figure 2. - Surface deformation of semi-infinite body subjected to uniform pressure over rectangular area.

$$D = b[(\bar{X} - B)\ \ln(\bar{X} - B)^2 - (\bar{X} + B)\ \ln(\bar{X} + B)^2 + 4B(1 - \ln b)] \tag{20}$$

and

b semiwidth of Hertzian contact

B $\bar{b}/b$

$\bar{b}$ b/n

n number of nodes within semiwidth of Hertzian contact

Now the term $\delta(\bar{x})$ in equation (19) represents the elastic deformation at a point $\bar{x}$ due to a rectangular area of uniform pressure p and width $2\bar{b}$. If the contact is divided into a number of equal rectangular areas, the total deformation at a point $\bar{x}$ due to the contributions of the various rectangular areas of uniform pressure in the contact can be evaluated numerically. The total elastic deformation caused by the rectangular areas of uniform pressure within a contact can be written as

$$\delta_k(x) = \frac{2}{\pi} \sum_{i=1,2,\ldots} P_i D_j \tag{21}$$

where

$$j = \left|k - i\right| + 1 \tag{22}$$

Therefore, substituting equations (17) and (21) into equation (16) while writing the film thickness in dimensionless form gives

$$H_k = \frac{h}{R} = H_o + \frac{1}{R}\left[\frac{X^2}{2}\left(\frac{b^2}{R}\right) + \frac{2}{\pi} \sum_{i=1,2,\ldots} P_i D_j\right] \tag{23}$$

Phi (Φ) Solution

Having defined the density and film thickness, we can return to the solution of the Reynolds equation. The dimensionless reduced pressure Q given in equation (14) plotted as a function of X exhibits a very localized pressure field with high values of dQ/dX and d^2Q/dX^2. Such a condition with high gradients is not welcomed when performing numerical analysis by relaxation methods. Therefore, as discovered by Hamrock and Dowson (ref. 5), to produce a much gentler curve, a parameter Φ is introduced, where

$$\Phi = QH^{3/2} = \frac{H^{3/2}(1 - e^{-GP})}{G} \tag{24}$$

The dimensionless reduced pressure Q is smaller at large values of film thickness H and large when the film thickness is small. The Φ substitution also has the advantage that it eliminates all terms containing deriva-

tives of products of H and Q or H and Φ. Therefore, from equation (24) while expanding terms within equation (14), we get

$$H^{3/2}\frac{d}{dx}\left(\frac{\bar{}}{\rho}\frac{d\Phi}{dx}\right) - \frac{3\Phi}{2}\frac{d}{dx}\left(\bar{\rho}H^{1/2}\frac{dH}{dx}\right) = 24U\sqrt{\frac{2W}{\pi}}\frac{d}{dx}(\bar{\rho}H) \tag{25}$$

The first step is then to replace equation (25) by a finite difference approximation. The relaxation method relies on the fact that a function can be represented with sufficient accuracy over a small range by a quadratic expression. With standard finite central-difference representation, equation (25) can be written as

$$A_i\Phi_{i+1} + C_i\Phi_{i-1} - L_i\Phi_i - M_i = 0 \tag{26}$$

where

$$A_i = 3\bar{\rho}_{i+1} + \bar{\rho}_{i-1} \tag{27}$$

$$C_i = \bar{\rho}_{i+1} + 3\bar{\rho}_{i-1} \tag{28}$$

$$L_i = 4(\bar{\rho}_{i+1} + \bar{\rho}_{i-1}) + \frac{1.5[\bar{\rho}_{i+1}\sqrt{H_{i+1}}(3H_{i+1} - 4H_i + H_{i-1}) + \bar{\rho}_{i-1}\sqrt{H_{i-1}}(H_{i+1} - 4H_i + 3H_{i-1})]}{H_i^{3/2}} \tag{29}$$

$$M_i = \frac{24U\sqrt{\frac{2W}{\pi}}\left(\frac{2}{n}\right)(\bar{\rho}_{i+1}H_{i+1} - \bar{\rho}_{i-1}H_{i-1})}{H_i^{3/2}} \tag{30}$$

Figure 3 shows the uniform placement of the nodes within the contact. This nodal structure was used in all of the results. The number of nodes within a semicontact width was 120 throughout all calculations.

The following boundary conditions have been adopted:

(1) At the inlet and outlet the pressure was set to zero. This implies that Q and Φ are also zero at these positions.

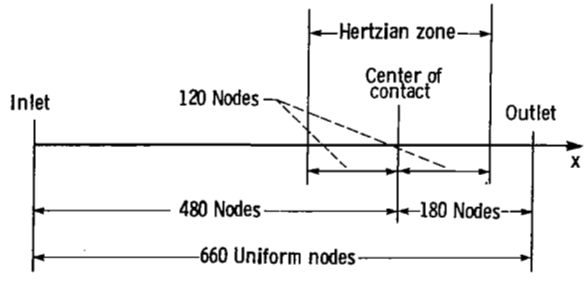

Figure 3. - Nodal structure for numerical calculations.

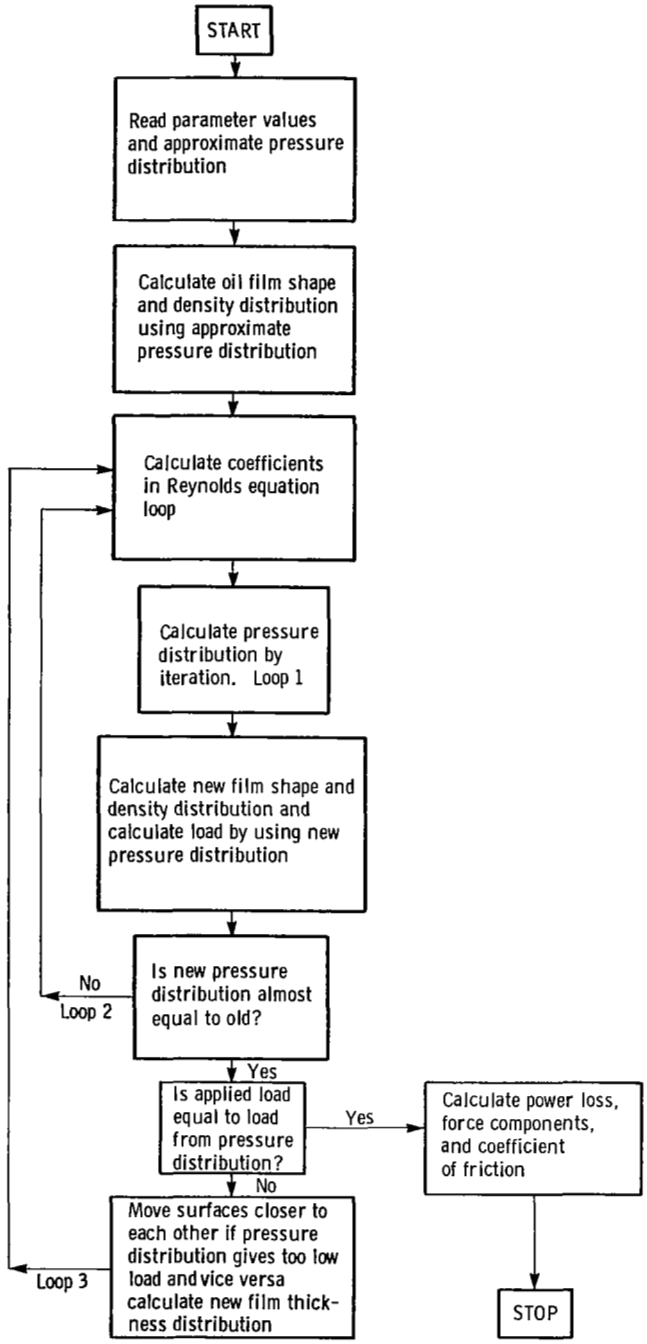

Figure 4. - Flow chart of computational procedures used in elastohydrodynamic lubrication studies.

(2) At the cavitation boundary

$$P = \frac{dP}{dX} = 0 \tag{31}$$

Equation (26) represents a system of simultaneous equations that was solved by the standard Gauss-Seidel iterative method. A flow chart shown in figure 4

describes the computational procedures used in the elastohydrodynamic lubrication studies.

Mass Flow Rate Per Unit Length

The mass flow rate per unit length for elastohydrodynamically lubricated contacts can be written as

$$k = u\rho h - \frac{\rho h^3}{12\eta}\frac{dp}{dx} \tag{32}$$

Making use of equation (2) while rearranging terms gives

$$k = \left(\frac{\rho_0 E' R^2}{12\ \eta_0}\right)(\bar{\rho}H)\left(12U - \frac{H^2}{2\bar{\eta}}\sqrt{\frac{\pi}{2W}}\frac{dP}{dX}\right) \tag{33}$$

Making use of equation (13) allows this equation to be rewritten as

$$K = \frac{k}{\rho_0 UR} = \bar{\rho}H\left(1 - \frac{H^2}{24U}\sqrt{\frac{\pi}{2W}}\frac{dQ}{dX}\right) \tag{34}$$

The second term on the right side of equation (34) is the Poiseuille or pressure term. Writing the reduced pressure gradient in equation (34) in a central difference form and rearranging the terms, we get

$$Q_{i+1} = Q_{i-1} + 24U\sqrt{\frac{2W}{\pi}}\left(\frac{2}{n}\right)\frac{1}{H_i^2}\left(1 - \frac{K_i}{\bar{\rho}_i H_i}\right) \tag{35}$$

This expression enables the reduced pressure to be written in terms of flow, film shape, and density at the preceding location.

Force Components

Figure 5 shows the force components acting on the two solids along with the film geometry in a portion of a concentrated contact. Conventionally only

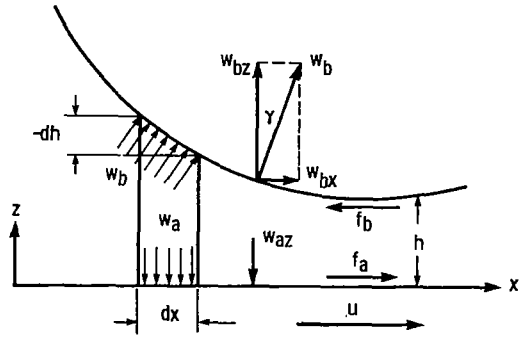

Figure 5. - Force components.

the z-components of the normal forces acting on the solids (w_{az} and w_{bz}) are considered. However, it was felt that the tangential x-components (w_{ax} and w_{bx}), shear forces (f_a and f_b), coefficient of friction μ, and center of pressure x_{cp} should also be expressed and quantitative values obtained for each of these expressions. The normal z-component of the force per unit length acting on the solids can be written as

$$w_z = w_{az} = w_{bz} = \int p \, dx \tag{36}$$

Using the dimensionalization given in equation (2) gives this equation as

$$W = \frac{w_z}{E'R} = \frac{b}{r} \int P \, dX = \frac{8}{\pi} \left(\int P \, dX \right)^2 \tag{37}$$

In equation (37) W is usually referred to as the dimensionless load parameter.

The tangential force component w_{ax} for solid a is zero. The tangential force component per unit length for solid b is not zero and can be written as

$$w_{bx} = - \int p \, dh = - \int p \frac{dh}{dx} \, dx \tag{38}$$

Using integration by parts gives

$$w_{bx} = -[ph]_i^o + \int h \frac{dp}{dx} \, dx \tag{39}$$

where i and o refer to inlet and outlet edge of the computing zone, respectively.

However, the pressure at the edge of the inlet and at the edge of the outlet is zero. Using the dimensionalization given in equation (2) gives

$$W_{bx} = \frac{w_{bx}}{E'R_x} = \int H \frac{dP}{dX} \, dX \tag{40}$$

The resulting force components per unit length can be written as

$$W_a = \frac{w_a}{E'R_x} = \sqrt{W_{ax}^2 + W_{az}^2} = W_{az} \tag{41}$$

$$W_b = \frac{w_b}{E'R_x} = \sqrt{W_{bx}^2 + W_{bz}^2} = \sqrt{W_{bx}^2 + W^2} \tag{42}$$

$$\gamma = \tan^{-1} \left(\frac{w_{bx}}{w_{bz}} \right) = \tan^{-1} \left(\frac{W_{bx}}{W} \right) \tag{43}$$

Shear Forces

The shear force per unit length acting on solid a (shown in fig. 5) can be written as

$$f_a = \int \left(\eta \frac{du}{dz}\right)_{z=0} dx \tag{44}$$

From Hamrock and Dowson (ref. 6, p. 141, eq. 5.30) we can write

$$\eta \frac{du}{dz} = \frac{(2z - h)}{2} \frac{dp}{dx} - \frac{\eta(u_a - u_b)}{h} \tag{45}$$

Substituting this equation into (44) gives

$$f_a = -\int \left[\frac{h}{2} \frac{dp}{dx} + \frac{\eta(u_a - u_b)}{h}\right] dx \tag{46}$$

Making use of equation (39) while writing equation (46) in dimensionless terms gives

$$F_a = -\frac{W_{bx}}{2} - \frac{4(u_a - u_b)}{(u_a + u_b)} U\sqrt{\frac{2W}{\pi}} \int \frac{\bar{\eta}}{H} dx \tag{47}$$

The shear force per unit length acting on solid b can be written as

$$f_b = \int \left(\eta \frac{du}{dz}\right)_{z=h} dx \tag{48}$$

Making use of equation (45) gives equation (48) as

$$F_b = \frac{W_{bx}}{2} - \frac{4(u_a - u_b)}{(u_a + u_b)} U\sqrt{\frac{2W}{\pi}} \int \frac{\bar{\eta}}{H} dx \tag{49}$$

Note that for equilibrium to be satisfied the following must be true:

$$F_a - F_b + W_{bx} = 0 \tag{50}$$

$$W_{az} - W_{bz} = 0 \tag{51}$$

The coefficient of friction is written as

$$\mu = -\frac{F_a}{W} = \frac{-F_b + W_{bx}}{W} \tag{52}$$

Center of Pressure

A calculation very useful in traction studies is the location of the center of pressure. The appropriate equation is

$$x_{cp} = \frac{1}{w_z} \int p x \, dx \tag{53}$$

Writing this in dimensionless form gives

$$X_{cp} = \frac{x_{cp}}{b} = \sqrt{\frac{\delta}{\pi W}} \int P X \, dX \tag{54}$$

The location of the center of pressure indicates the position on which the resulting force is acting. The fact that the resulting force is not acting through the center of the roller creates a rolling resistance in the form of a moment. This has a significant effect in the evaluation of the resulting forces and power loss in traction devices and other machine elements.

RESULTS

Dimensionless Grouping

From the variables of the numerical analysis the following dimensionless groups can be defined:

Dimensionless film thickness:

$$H = \frac{h}{R} \tag{55}$$

Dimensionless load parameter:

$$W = \frac{w_z}{E'R} \tag{56}$$

where w_z is the load per unit length.

Dimensionless speed parameter:

$$U = \frac{\eta_0 u}{E'R} \tag{57}$$

Dimensionless materials parameter:

$$G = \alpha E' \tag{58}$$

The dimensionless film thickness for a rectangular contact can thus be written as a function of the other three parameters:

$$H = f(W, U, G) \tag{59}$$

The most important practical aspect of elastohydrodynamic lubrication theory is the determination of the minimum film thickness within the contact. There-

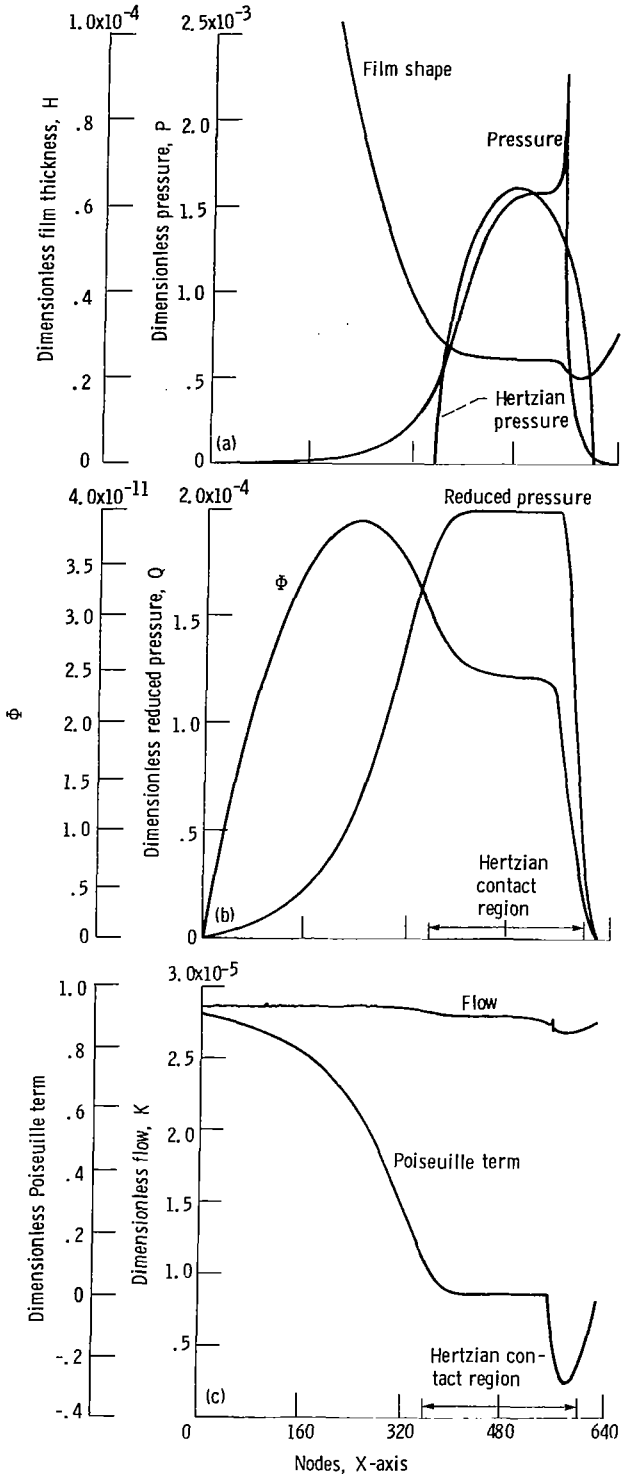

(a) Dimensionless pressure and film thickness.

(b) Dimensionless reduced pressure and Φ.

(c) Dimensionless flow and Poiseuille term.

Figure 6. - Representative variations of dimensionless pressure, film thickness, and reduced pressure, Φ, dimensionless flow, and the Poiseuille term on x-axis for dimensionless speed parameter U of $1x10^{-11}$ dimensionless load parameter W of $1.638x10^{-5}$, and dimensionless materials parameter G of 5000.

fore, in the fully flooded results to be presented, the dimensionless parameters (W, U, and G) will be varied and the effect on the minimum film thickness will be studied.

Representative variations of dimensionless pressure, film thickness, reduced pressure, Φ, dimensionless flow, and the Poiseuille term on the X-axis are shown in figure 6. Figure 6(a) shows the variation of dimensionless pressure and film thickness on the X-axis for $U = 1.0\times10^{-11}$, $W = 1.638\times10^{-5}$, and $G = 5000$. The inlet region is to the left and the outlet is to the right in this and each of the remaining figures to be presented. The Hertzian pressure is also shown in this figure. The characteristic pressure spike is clearly evident in this figure as is the parallel film shape through the central part of the contact, with a minimum film occurring near the outlet of the contact.

Variation of dimensionless reduced pressure Q and Φ on the X-axis for $U = 1.0\times10^{-11}$, $W = 1.638\times10^{-5}$, and $G = 5000$ is shown in figure 6(b). Recall that the reduced pressure is defined in equation (12) and Φ in equation (24). Figure 6(b) shows that the reduced pressure Q is constant within the contact and that Φ is constant in part of the contact outlet.

Figure 6(c) shows the variation of dimensionless flow and the Poiseuille term on the X-axis for $U = 1.0\times10^{-11}$, $W = 1.638\times10^{-5}$, and $G = 5000$. Equation (34) defines the mass flow rate per unit length, and the Poiseuille term is the reduced pressure gradient term of equation (34). In figure 6(c) the flow is constant throughout the contact. Great care was taken to assure that this was true for all the results to be presented. Slight adjustments in the pressure profile were necessary in the inlet region to assure that the flow was constant in that region. The Poiseuille term approaches 1 at the inlet and zero in the Hertzian contact region except for having negative values from the pressure spike to the outlet.

Influence on Load

Changes in the dimensionless load parameter W can be achieved while keeping the other parameters constant by changing only the normal applied load per unit length w_z in equation (56). The values at which the remaining parameters U and G were held constant during the calculations were

$$U = 1.0\times10^{-11}$$
$$G = 5000 \qquad (60)$$

Four values of the dimensionless load parameter W and the corresponding values of minimum film thickness H_{min} obtained from the elastohydrodynamic lubrication theory developed earlier are shown in table I. These four pairs of data were used to determine an empirical relationship between the dimensionless load and the minimum film thickness.

$$\overline{H}_{min} = C_1 W^{C_2} \qquad (61)$$

By applying a least-squares power fit to the four pairs of data $[(W_i, H_{min,i}), i = 1,\ldots,4]$, the values of C_1 and C_2 were found to be $C_1 = 6.33\times10^{-6}$ and $C_2 = -0.1056 \simeq -0.11$. Therefore the influence of load on minimum film thickness can be written as

$$\bar{H}_{min} \propto W^{-0.11} \tag{62}$$

In addition to the least-squares fit, a coefficient of determination ε was obtained. The value of ε reflects the fit of the data to the resulting equation: unity representing a perfect fit, and zero the worst possible fit. The coefficient of determination ε for these results was 0.9856, which is excellent.

Figure 7 shows the variation of dimensionless pressure and film thickness on the X-axis for two values of dimensionless load W (1.638×10^{-5} and 3.0×10^{-5}). The values of the dimensionless speed and materials parameters were held fixed as described by equation (60). Figure 7 shows that although the pressure distribution changes considerably, the minimum film thickness is only slightly affected. This illustrates the slight effect of the dimensionless load parameter W on minimum film thicknesses, as described in equation (62).

Influence of Speed

If the surface velocity in the x-direction is changed, the dimensionless speed parameter U is modified as shown in equation (57), but the other dimensionless parameters (W and G) remain constant. The values at which these dimensionless parameters were held constant in the calculations performed to determine the influence of speed on film thickness were

$$\left.\begin{aligned} W &= 2.048 \times 10^{-5} \\ G &= 5000 \end{aligned}\right\} \tag{63}$$

Values of the dimensionless speed parameter U and the corresponding minimum film thickness H_{min} as obtained from the elastohydrodynamic lubrication of rectangular contacts developed earlier in the report are presented in

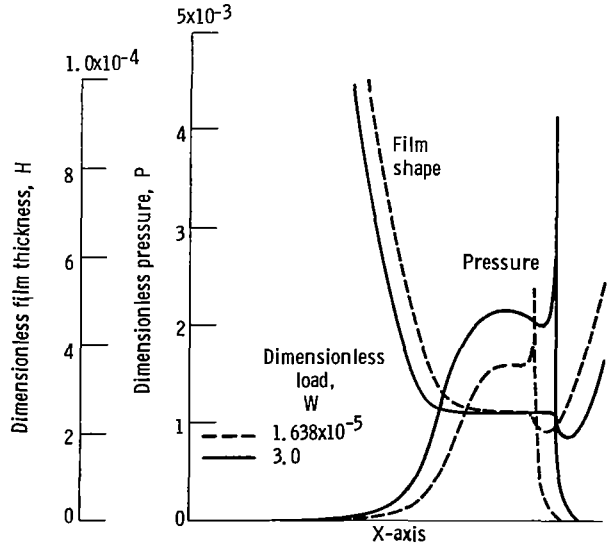

Figure 7. - Variation of dimensionless pressure and film thickness on X-axis for two values of dimensionless load.

table II. Calculations were performed for five values of dimensionless speed parameter covering nearly an order of magnitude. The solutions enabled the relationship between minimum film thickness and the speed parameter to be written in the form

$$\overline{H}_{min} = C_3 U^{C_4} \tag{64}$$

By applying a least-squares power fit to the five pairs of data $[(U_i, \overline{H}_{min,i}), i = 1, \ldots, 5]$, the values of C_3 and C_4 were found to be $C_3 = 1179.2$ and $C_4 = 0.70640 \approx 0.71$. The coefficient of determination ϵ for these results was excellent at 0.9992. Therefore the influence of speed on minimum film thickness can be written as

$$\overline{H}_{min} \propto U^{0.71} \tag{65}$$

Figure 8 shows the variation of dimensionless pressure and film thickness on the X-axis for two values of dimensionless speed U ($0.5\text{x}10^{-11}$ and $3.0\text{x}10^{-11}$). The values of the dimensionless load and materials parameters were held fixed as described by equation (63). This figure shows that the pressure at any location in the inlet region rises in going from the lower speed to the higher speed. This result is consistent with the elastohydrodynamic lubrication theory of elliptical contact given by Hamrock and Dowson (ref. 5). Note that the pressure spike moves more toward the outlet for the lower speed than for the higher speed. A typical elastohydrodynamic film shape with an essentially parallel section in the central region is also shown in figure 8. There is a considerable change in film thickness as the dimensionless speed is changed, as indicated by equation (65). This illustrates most clearly the dominant effect of the dimensionless speed parameter U on the minimum film thickness in elastohydrodynamically lubricated contacts.

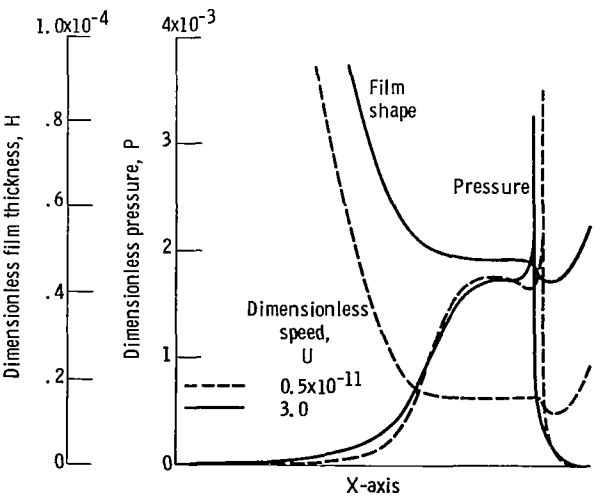

Figure 8. - Variation of dimensionless pressure and film thickness on X-axis for two values of dimensionless speed.

Influence of Material Properties

A study of the influence of the dimensionless materials parameter G on minimum film thickness has to be approached with caution since in practice it is not possible to change the physical properties of the materials, and hence the value of G, without influencing the other dimensionless parameters considered earlier. Equations (56) to (58) show that as either the materials of the solids (as expressed in E') or the lubricant (as expressed in η_0 and α) are varied, not only does the materials parameter G change, but so do the dimensionless speed U and load W parameters.

The results obtained from calculations performed for three values of the dimensionless materials parameter are summarized in table III. A general form of these results, showing how the minimum film thickness is a function of the dimensionless materials parameter, is written as

$$T = C_5 G^{C_6} \tag{66}$$

where

$$T = \frac{H_{min}}{U^{0.71} W^{-0.11}} \tag{67}$$

In equation (67) the exponents have been rounded off to two significant figures so that any error would be absorbed in C_5, given in equation (66). By applying a least-squares power fit to the three pairs of data, the values of C_5 and C_6 were found to be $C_5 = 3.12$ and $C_6 = 0.5670 \simeq 0.57$. The coefficient of determination for these results was 0.9969, which is excellent. Therefore the effect of the dimensionless materials parameter on minimum film thickness can be written with adequate accuracy as

$$\bar{H}_{min} \propto G^{0.57} \tag{68}$$

Minimum-Film-Thickness Formula

The proportionality equations (62), (65), and (68) have established how the minimum film thickness varies with the load, speed, and materials parameters, respectively. This enables a composite dimensionless minimum-filmthickness formula for a fully flooded, isothermal elastohydrodynamic rectangular contact to be written as

$$\boxed{\bar{H}_{min} = 3.07\, U^{0.71} G^{0.57} W^{-0.11}} \tag{69}$$

In equation (69) the constant 3.07 is different from $C_5 = 3.12$ mentioned earlier to account for the rounding off of the materials-parameter exponent. In dimensional terms this equation is written as

$$\bar{h}_{min} = 3.07 \frac{\alpha^{0.57} R^{0.4} (u\eta_0)^{0.71}}{(E')^{0.03} w_z^{0.11}} \tag{70}$$

From this equation we find that the minimum film thickness depends inversely on the effective elastic modulus E' and load per unit length w_z. Both have small exponents, indicating that the minimum film thickness h_{min} is only slightly affected by the effective elastic modulus and load per unit length. In contrast to these effects from equation (70) we find that the film thickness depends directly on the pressure-viscosity coefficient of the lubricant α, the geometry R, the surface velocity in the direction of motion u, and the viscosity at atmospheric pressure η_0. From the values of the exponents on these parameters (α, R, u, and η_0) it is clear that they have a dominating effect on the minimum film thickness.

It is interesting to compare equation (69) with earlier derived minimum-film-thickness formulas. Dowson and Higginson (ref. 9) obtained the following expression:

$$(\bar{H}_{min})_{DH} = 1.6\, U^{0.7} G^{0.6} W^{-0.13} \tag{71}$$

It was found that this equation produced a positive exponent on the effective elastic modulus, which is contrary to physical intuition. This equation was therefore revised by Dowson (ref. 7) as

$$(\bar{H}_{min})_{D} = 2.65\, U^{0.7} G^{0.54} W^{-0.13} \tag{72}$$

The powers of U, G, and W in equations (69) and (72) are quite similar considering the different numerical procedures on which they are based.

The Hamrock and Dowson (ref. 11) ellipical contact minimum-film-thickness formula for very long elliptical contacts, where the ellipticity parameter is large and the elliptical contact approaches a rectangular contact, is expressed as

$$(\bar{H}_{min})_{HD} = 3.63\, U^{0.68} G^{0.49} W^{-0.073} \tag{73}$$

It is interesting to compare equation (73) with equation (69). The powers of U, G, and W are again seen to be quite similar.

Table IV gives the 10 cases used in obtaining equation (69). In this table H_{min} corresponds to the minimum film thickness obtained from the elastohydrodynamic lubrication rectangular contact theory developed earlier in this report and $\bar{H}_{min}$ is the minimum film thickness obtained from equation (69). The percentage difference between these two values is expressed by V_1, which is defined as

$$V_1 = \left(\frac{\bar{H}_{min} - H_{min}}{H_{min}} \right) 100 \tag{74}$$

In table IV the values of V_1 are within ±2 percent. The dimensionless minimum film thickness obtained by Dowson (ref. 7) and expressed in equation (72) is also shown in table IV as $(\bar{H}_{min})_D$. The percentage

difference between this film thickness and that of H_{min} is expressed by V_2, where

$$V_2 = \left[\frac{(H_{min})_D - H_{min}}{H_{min}}\right] 100 \tag{75}$$

In table IV the values of V_2 are within +4 to +8 percent, meaning that the Dowson (ref. 7) formula produces 4 to 8 percent larger film thickness than that obtained from the present analysis.

Figure 9 compares the pressure profile as obtained from Dowson and Higginson (ref. 9) with the present results for $U = 1.0\times10^{-11}$, $W = 3.0\times10^{-5}$, and $G = 5000$. The Hertzian pressure is also shown in this figure. The Dowson and Higginson (ref. 9) profile is exactly equivalent to the Hertzian pressure for most of the contact region, but the present results are somewhat lower than the Hertzian pressure. The pressure spike is higher in magnitude in the present results and located farther away from the exit of the contact than in the results obtained by Dowson and Higginson (ref. 9).

Table V shows the values of the load components, the coefficient of friction, and the location of the center of pressure for the 10 cases presented in table IV. The values of the dimensionless load, speed, and materials parameters corresponding to a particular case can be obtained from table IV. Table V shows that the tangential force components are three orders of magnitude less than the normal force components. Also the coefficient of friction decreases with increasing load and increases with increasing speed. Table V gives values of the location of the center of pressure for the 10 cases evaluated. In all the cases the center of pressure is in front of the center of the Hertzian contact. An approximate formula for the location of the center of pressure is a function of the dimensionless load and speed and is given as

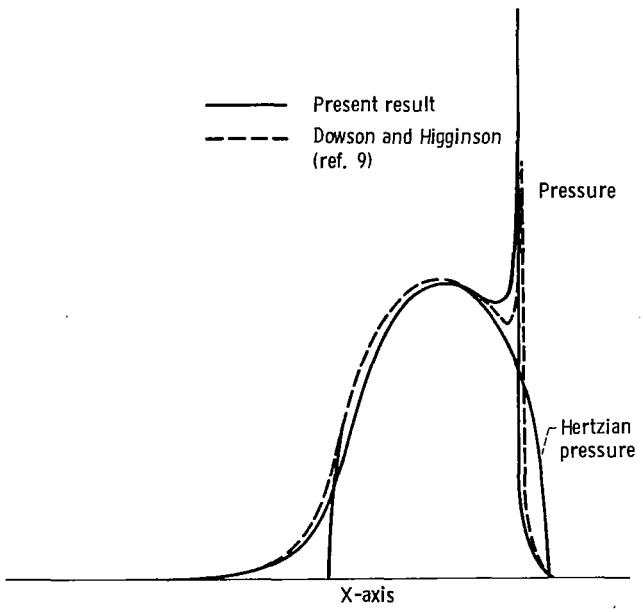

Figure 9. - Comparison of pressure profile of present results with that of Dowson and Higginson (ref. 9).

$$\bar{X}_{cp} = -0.05\ U^{0.44}W^{-1.13} \qquad (76)$$

where $\bar{X}_{cp}$ is measured from the center of the Hertzian contact. This formula was obtained by using the data in table V and is valid only for steel surfaces. The value obtained from the approximate expression of the location of the center of pressure (eq. (76)) is shown in the last column of table V. The maximum error in calculating the location of the center from equation (76) as compared with the exact solution is 0.89 percent of the Hertzian half width, which is excellent. Using equation (76) for bronze surfaces gives an error of up to 3.54 percent of the Hertzian half width. This larger error is due to having only two cases of bronze material in the formulation of the expression.

CONCLUDING REMARKS

A procedure for the numerical solution of the complete isothermal elastohydrodynamic lubrication problem for rectangular contacts has been outlined. This procedure calls for the simultaneous solution of the elasticity and Reynolds equations. In the elasticity analysis the conjunction was divided into equal rectangular areas. It was assumed that a uniform pressure was applied over each element. In the numerical analysis of the Reynolds equation the parameter $\Phi = QH^{3/2}$ was introduced in order to help the relaxation process. The analysis coupled the elasticity and Reynolds equations, going from the inlet to the outlet without making any assumptions other than neglecting side leakage.

By using the procedures outlined in the analysis the influence of the dimensionless speed U, load W, and materials G parameters on minimum film thickness was investigated. Ten cases were used to generate the minimum-film-thickness relationship

$$\bar{H}_{min} = 3.07\ U^{0.71}G^{0.57}W^{-0.11}$$

The most dominant exponent occurred in association with the speed parameter; the exponent on the load parameter was very small and negative. The materials parameter also carried a significant exponent, although the range of the parameter in engineering situations is limited. The five dimensionless speed parameter values used in obtaining the preceding equation were varied over a range six times the lowest speed value. The four dimensionless load values were varied over a range 1.8 times the lowest load value. Conditions corresponding to the use of solid materials of bronze and steel and lubricants of paraffinic and naphthenic mineral oils were considered in obtaining the exponent in the dimensionless materials parameter.

Plots were presented that indicate in detail the pressure distribution, film shape, and flow within the contact. The characteristic pressure spike was clearly in evidence as was the parallel film shape through the central portion of the contact. Minimum film thickness occurred near the outlet of the contact.

National Aeronautics and Space Administration
Lewis Research Center
Cleveland, Ohio, August 5, 1982

REFERENCES

1. Meldahl, A.: Contribution to Theory of Lubrication of Gears and of Stressing of Lubricated Flanks of Gear Teeth. Brown Boveri Rev., vol. 28, no. 11, Nov. 1941, pp. 374–382.

2. Grubin, A. N.; and Vinogradova, I. E.: Fundamentals of the Hydrodynamic Theory of Lubrication of Heavily Loaded Cylindrical Surfaces. Investigation of the Contact Machine Components, Kh. F. Ketova, ed., Translation of Russian Book No. 30, Central Scientific Institute for Technology and Mechanical Engineering, 1949, Chapter 2. (Available from Dept. of Scientific and Industrial Research. Great Britain, transl. CTS-235, and from Special Libraries Association, Chicago, transl. R-3554).

3. Dowson, D.; and Higginson, G. R.: New Roller-Bearing Lubrication Formula. Engineering (London), vol. 192, no. 4972, Aug. 1961, pp. 158–159.

4. Jacobson, B. O.: On the Lubrication of Heavily Loaded Spherical Surfaces Considering Surface Deformations and Solidifications of the Lubricant. Acta Polytech. Scand., Mech. Eng. Ser., no. 54, 1970.

5. Hamrock, B. J.; and Dowson, D.: Isothermal Elastohydrodynamic Lubrication of Point Contacts. Part I – Theoretical Formulation. J. Lubr. Technol., vol. 98, no. 2, Apr. 1976, pp. 223–229.

6. Hamrock, B. J.; and Dowson, D.: Ball Bearing Lubrication – The Elastohydrodynamics of Elliptical Contacts. John Wiley & Sons, Inc., 1981.

7. Dowson, D.: Elastohydrodynamics. Proc. Inst. Mech. Eng., London, vol. 182(3A), 1968, pp. 151–167.

8. Barus, C.: Isotherms, Isopiestics, and Isometrics Relative to Viscosity. Am. J. Sci., vol. 45, 1893, pp. 87–96.

9. Dowson, D.; and Higginson, G. R.: Elastohydrodynamic Lubrication – The Fundamentals of Roller and Gear Lubrication. Pergamon Press, 1966.

10. Timoshenko, S.; and Goodier, J. N.: Theory of Elasticity. 2nd ed., McGraw-Hill Book Co., 1951.

11. Hamrock, B. J.; and Dowson, D.: Isothermal Elastohydrodynamic Lubrication of Point Contacts. Part III – Fully Flooded Results. J. Lubr. Technol., vol. 99, no. 2, Apr. 1977, pp. 264–276.

TABLE I. - EFFECT OF DIMENSIONLESS LOAD PARAMETER ON MINIMUM FILM THICKNESS

Force per unit length, w_z, N/m	Dimensionless load, W	Dimensionless film thickness, H_{min}
40 000.0	1.6382×10^{-5}	20.327×10^{-6}
50 000.0	2.0478	19.711
60 000.0	2.4573	19.396
73 249.3	3.0000	19.055

TABLE II. - EFFECT OF DIMENSIONLESS SPEED PARAMETER ON MINIMUM FILM THICKNESS

Surface velocity, u, m/s	Dimensionless speed, U	Dimensionless film thickness, H_{min}
0.297040	0.5×10^{-11}	12.357×10^{-6}
.415856	.7	15.482
.594080	1.0	19.711
1.188160	2.0	33.364
1.782240	3.0	43.029

TABLE III. - EFFECT OF DIMENSIONLESS MATERIALS PARAMETER ON MINIMUM FILM THICKNESS

Solid material	Lubricant	Dimensionless materials parameter, G	Dimensionless speed parameter, U	Dimensionless load parameter, W	Minimum film thickness from EHL rectangular theory, H_{min}	$T = \frac{H_{min}}{U^{0.71} W^{-0.11}}$
Bronze	Paraffinic	2553.7	1.9579×10^{-11}	4.0094×10^{-5}	20.156×10^{-6}	265.20
Bronze	Naphthenic	3591.1	5.5975	4.0094	52.502	327.67
Steel	Paraffinic	5000.0	1.0000	2.0478	19.711	388.11

TABLE IV. - EFFECT OF DIMENSIONLESS LOAD, SPEED, AND MATERIALS PARAMETERS ON MINIMUM FILM THICKNESS

Case	Dimensionless load parameter, W	Dimensionless speed parameter, U	Dimensionless materials parameter, G	Dimensionless film thickness obtained from EHL theory, H_{min}	Dimensionless film thickness obtained from least-squares fit, $\bar{H}_{min}$	Percentage difference between H_{min} and $\bar{H}_{min}$, V_1	Dimensionless film thickness obtained from Dowson (ref. 7), $(\bar{H}_{min})_D$	Percentage difference between $\bar{H}_{min}$ and $(\bar{H}_{min})_D$, V_2
1	1.6382×10^{-5}	1.0000×10^{-11}	5000.0	20.327×10^{-6}	20.510×10^{-6}	0.900	22.020×10^{-6}	7.362
2	2.0478	↓	↓	19.711	20.013	1.532	21.391	6.886
3	2.4573			19.396	19.616	1.134	20.890	6.495
4	3.0000			19.055	19.189	.703	20.355	6.076
5	2.0478	.50000		12.357	12.235	-.987	13.167	7.617
6	2.0478	.70000		15.482	15.536	.349	16.664	7.261
7	2.0478	2.0000		33.364	32.737	-1.879	34.749	6.146
8	2.0478	3.0000		43.029	43.658	1.462	46.154	5.717
9	4.0094	1.9579	2553.7	20.156	20.420	1.310	21.826	6.885
10	4.0094	5.5975	3591.1	52.502	52.283	-.417	54.735	4.690

TABLE V. - VALUES OF LOAD COMPONENTS, COEFFICIENT OF FRICTION, AND LOCATION OF CENTER OF PRESSURE FOR 10 CASES EVALUATED

Case	Dimensionless normal load, W	Dimensionless tangential load, W_{bx}	Coefficient of friction, μ	Dimensionless center of pressure, X_{cp}	Dimensionless center of pressure obtained from least-squares fit, $\bar{X}_{cp}$
1	1.6382×10^{-5}	2.0221×10^{-8}	6.1716×10^{-4}	-0.1912	-0.1881
2	2.0478	2.2939	5.6008	-.1552	-.1463
3	2.4573	2.4071	4.8979	-.1240	-.1191
4	3.0000	2.5448	4.2414	-.0971	-.0951
5	2.0478	1.5388	3.7572	-.1041	-.1080
6	2.0478	1.7647	4.3087	-.1194	-.1251
7	2.0478	2.7985	6.8330	-.1893	-.1982
8	2.0478	3.4243	8.3609	-.2317	-.2367
9	4.0094	4.1764	5.2082	-.1031	-.0921
10	4.0094	7.3268	9.1369	-.1810	-.1456

1. Report No. NASA TP-2111	2. Government Accession No.	3. Recipient's Catalog No.
4. Title and Subtitle ELASTOHYDRODYNAMIC LUBRICATION OF RECTANGULAR CONTACTS		5. Report Date January 1983 6. Performing Organization Code 505-32-42
7. Author(s) Bernard J. Hamrock and Bo O. Jacobson		8. Performing Organization Report No. E-1277 10. Work Unit No.
9. Performing Organization Name and Address National Aeronautics and Space Administration Lewis Research Center Cleveland, Ohio 44135		11. Contract or Grant No. 13. Type of Report and Period Covered Technical Paper
12. Sponsoring Agency Name and Address National Aeronautics and Space Administration Washington, D. C. 20546		14. Sponsoring Agency Code

15. Supplementary Notes

Bernard J. Hamrock, Lewis Research Center; Bo O. Jacobson, University of Luleå, Luleå, Sweden, and National Research Council - NASA Research Associate.

16. Abstract

The analysis of isothermal elastohydrodynamically lubricated rectangular contact was evaluated numerically. This required the simultaneous solution of the elasticity and Reynolds equations. In the elasticity analysis the contact zone was divided into equal rectangular areas, and it was assumed that a uniform pressure was applied over each area. The elastohydrodynamic lubrication theory thus developed was used to investigate the influence of the dimensionless speed, load, and materials parameters on minimum film thickness. Ten cases were used in obtaining the minimum-film-thickness formula

$$\bar{H}_{min} = 3.07\, U^{0.71} G^{0.57} W^{-0.11}$$

Plots are shown that indicate the details of the pressure distribution, film shape, and flow. The characteristic pressure spike is clearly in evidence as is the parallel film shape through the central portion of the contact, with a minimum film thickness occurring near the outlet of the contact.

17. Key Words (Suggested by Author(s))

Elastohydrodynamic lubrication
Rolling element bearing lubrication
Lubrication of nonconformal contacts

18. Distribution Statement

Unclassified - unlimited
STAR Category 37

19. Security Classif. (of this report)	20. Security Classif. (of this page)	21. No. of Pages	22. Price*
Unclassified	Unclassified	29	A03

* For sale by the National Technical Information Service, Springfield, Virginia 22161

NASA-Langley, 1983

8 1 1U,D, 830118 S00903DS
DEPT OF THE AIR FORCE
AF WEAPONS LABORATORY
ATTN: TECHNICAL LIBRARY (SUL)
KIRTLAND AFB NM 87117